Journal of Power Sources 222 (2013) 510–517

Contents lists available at SciVerse ScienceDirect

Journal of Power Sources

journal homepage: www.elsevier.com/locate/jpowsour

Fabrication of Pd/TiO_2-multiwall carbon nanotubes catalyst and investigation of its electrocatalytic activity for formic acid oxidation

Dandan Zhou, Liang Ding, Hao Cui, Hao An, Jianping Zhai, Qin Li*

State Key Laboratory of Pollution Control and Resource Reuse, School of the Environment, 22 Hankou Road, Nanjing University, Nanjing, Jiangsu 210046, PR China

HIGHLIGHTS

- TiO_2 was pretreated by 0.5 M HNO_3 to enhance its conductivity.
- TiO_2 was applied as support between Pd and MWNTs template.
- The introduction of TiO_2 promotes the Pd dispersion and decrease the Pd size.
- The application of TiO_2 as support highly improved the electrocatalytic activity and stability of the catalyst.
- The Pd/TiO_2-MWNTs shows great electrocatalytic ability for formic acid oxidation.

GRAPHICAL ABSTRACT

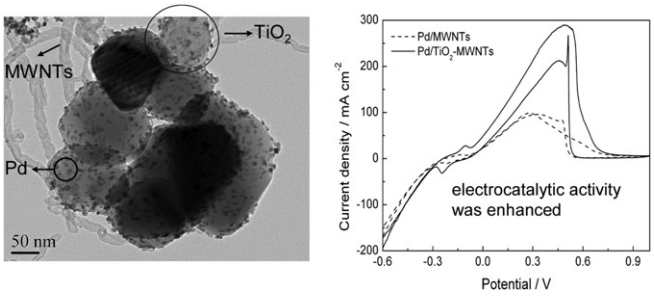

ARTICLE INFO

Article history:
Received 3 July 2012
Received in revised form
6 September 2012
Accepted 8 September 2012
Available online 14 September 2012

Keywords:
Titanium dioxide
Palladium
Multiwall carbon nanotubes
Formic acid oxidation
Electrocatalyst

ABSTRACT

In this study, a novel Pd/TiO_2-MWNTs catalyst is synthesized by a unique chemical method. The pretreated TiO_2 nanoparticles are applied as support materials between Pd nanoparticles and functional multiwall carbon nanotubes (MWNTs) template. The morphology and physicochemical properties of the catalysts are characterized by transmission electron microscopy (TEM), X-ray diffraction (XRD), and X-ray photoelectron spectroscopy (XPS). It is observed that the functional MWNTs are partially covered by TiO_2 nanoparticles, and that the metallic Pd nanoparticles are homogeneously deposited onto the TiO_2 nanoparticles with smaller sizes compared with those of Pd/MWNTs. The electrocatalytic activity of the Pd/TiO_2-MWNTs is investigated by cyclic voltammetry and chronoamperometry measurements in 0.5 M H_2SO_4 and 1 M HCOOH acidic solution, respectively. Results indicate that the introduction of pretreated TiO_2 into the nanocomposite highly improves its electrocatalytic activity, durability, and stability. Thus, the Pd/TiO_2-MWNTs catalyst is expected to be an effective electrode material for formic acid oxidation.

1. Introduction

The synthesis and applications of high electrocatalytic activity metal catalysts have attracted great attention in recent decades [1,2]. Among these, noble metal group catalysts are widely employed in the field of applied electrochemistry [3,4]. Although palladium shows high catalytic activity and low cost among the noble metal group [5], naked palladium nanoparticles are prone to aggregate, restricting their electrocatalytic activity. Currently, template supports with large superficial areas, such as carbon nanotubes, graphene, humic acid, are used to support palladium nanoparticles to prevent their aggregation [6,7].

Research on the application of oxide nanoparticles as support materials between catalytic nanoparticles and templates has recently seen great activity [8,9]. These studies have indicated that the addition of oxide nanoparticles in catalysts can not only enhance the durability and catalytic activity of the catalysts, but also improve their corrosion resistance and lower the degradation

* Corresponding author. Tel./fax: +86 25 83592903.
E-mail addresses: qinli_nju@yahoo.cn, qinli_nju@yahoo.com.cn (Q. Li).

0378-7753/$ – see front matter © 2012 Elsevier B.V. All rights reserved.
http://dx.doi.org/10.1016/j.jpowsour.2012.09.022

of their active surface area [10,11]. Among the many possible oxides, considerable attention has been paid to TiO_2 nanoparticles because of their long-term stability, nontoxicity, commercial availability, easy fabrication, and multifunctionality [12,13]. However, TiO_2 is a semiconductor with wide band gaps of 3.0 eV for the rutile and 3.2 eV for the anatase structures [14]. Therefore, to apply TiO_2 as catalyst, it is necessary to improve its electronic conductivity. Because of their good electrochemical stability, extraordinary electrical conductivity, robust mechanical strength, long aspect ratio, and large superficial area, carbon nanotubes are suitable as a template material for loading of nanocomposites [15,16]. TiO_2-CNTs nanocomposites are widely used as support materials in the large areas of optoelectronics and photocatalysis [17,18]. However, few researchers have reported on their electrocatalytic activity. It is supposed that the application of pretreated TiO_2-MWNTs as a support material for the loading of catalytic palladium nanoparticles could enhance their electrocatalytic activity and stability.

In recent years, great attention has been paid to direct formic acid fuel cells (DFAFCs) because of their many advantages such as limited fuel crossover, low toxicity, and high practical power densities at low temperature [19,20]. Research has found that Pd-based catalysts show great electrocatalytic activity for formic acid oxidation [19,21]. Therefore, in our experiments, we demonstrate a new method to synthesize Pd/TiO_2-MWNTs catalyst, and apply it to formic acid oxidation. The morphology and composition of the samples were characterized by transmission electron microscopy (TEM), X-ray diffraction (XRD), and X-ray photoelectron spectroscopy (XPS). In addition, the electrocatalytic activity of the Pd/TiO_2-MWNTs was investigated by cyclic voltammetry and chronoamperometry measurements.

2. Experimental section

2.1. Raw materials

Commercial MWCNTs (Nanotech Port Co., Shenzhen, China) were used in this work. All of the following materials were used as received: titanium tetrachloride ($TiCl_4$), palladium chloride ($PdCl_2$), concentrated nitric acid (HNO_3), concentrated sulfuric acid (H_2SO_4), sodium borohydride ($NaBH_4$), ethylene glycol, ethanol, formic acid, and isopropyl alcohol. These chemicals were all analytical grade and no purification was needed. All electrochemical experiments were carried out at room temperature. Ultrapure water was used throughout.

2.2. Pretreatment of MWNTs

MWNTs require pretreatment to avoid agglomeration and increase their dispersibility and surface functional groups. Typically, MWNTs were added to a 50 mL flask with concentrated HNO_3 and H_2SO_4 (1:3, v/v) under constant stirring at 80 °C for 10 h. Then, the mixture was filtered and washed with ultrapure water until the pH reached neutral. The resulting functional MWNTs were dried in an oven at 70 °C.

2.3. Fabrication and pretreatment of TiO_2

Titanium dioxide (TiO_2) nanoparticles were prepared by hydrolysis. First, titanium tetrachloride ($TiCl_4$) was rapidly dispersed in ethanol solvent with ultrasound treatment. A small amount of water was then added to the mixture and sonication was continued. After hydrolysis this mixture was dried at 110 °C. The resulting sample was washed with ethanol and ultrapure water, and collected by filtration. The sample was then dried at 500 °C in a muffle furnace for 3 h. Then, 0.5 M HNO_3 was added and the sample was dried at 500 °C for a further 1 h. Afterward, the sample was treated with 0.5 M HNO_3 for 4 h with strong stirring to avoid agglomeration and thereby improve its electronic conductivity. Last, the precipitate was filtered and washed with ultrapure water several times until the pH of the filtrate reached neutral, and dried at 70 °C.

2.4. Preparation of TiO_2-MWNTs and Pd/TiO_2-MWNTs catalysts

TiO_2-MWNTs were synthesized by an in-situ chemical method. First, 20 mg pretreated TiO_2 powder was dispersed in ultrapure water in a 100 mL beaker and ultrasonicated for 20 min. 10 mg functional MWNTs were added to the suspension with ultrasound treatment for another 30 min to obtain a uniform solution. Then, isopropyl alcohol was added to the mixture. After additional stirring for 30 min, ethylene glycol was dispersed in the solution and the resulting suspension was stirred for another 6 h to ensure the completion of the reaction. Finally, the sample was filtered and washed several times with ultrapure water, and dried at 70 °C.

Pd/TiO_2-MWNTs composite was synthesized using a borohydride reduction method. 4 mg $PdCl_2$ was sonicated at 50 °C for 30 min to obtain a uniform solvent. 20 mg TiO_2-MWNTs was dissolved in ultrapure water while being stirred, after which the Pd solution was added drop by drop. To reduce the Pd precursor, $NaBH_4$ was dissolved in ultrapure water and rapidly dropped into the solution while being vigorously stirred for another 8 h. The precipitate was filtered and washed several times with ultrapure water and then dried at 70 °C.

2.5. Electrochemical instrumentation and characterization

The size and morphology of these samples were observed by transmission electron microscopy (TEM, JEOL JEM-200CX), specimens for TEM observation were prepared by placing a drop of the particle-dispersed ethanol solution onto a copper grid. The crystal phases of these samples were analyzed by X-ray diffraction using Cu Kα radiation (XRD, ARL X'TRA). The data were collected for scattering angles (2θ) between 20° and 80° with a step size of 0.02°. The element states in the catalysts were analyzed by X-ray photoelectron spectroscopy (XPS, ULVAC-PHI PHI 5000 VersaProbe).

The electrocatalytic activity of the samples was investigated by cyclic voltammetry using a Model CHI 660D electrochemical workstation. A three-electrode cell was used in the electrochemical measurements. A glassy carbon (GC) electrode was used as the working electrode, a platinum foil (1 cm^2) was used as the counter-electrode, and a saturated potassium chloride electrode was used as the reference. 10 mg of the catalyst was homogeneously ultrasonically dispersed into 10 mL ultrapure water, after which 6 μL of the catalyst solution was dropped onto the GC electrode, and dried using infrared light.

3. Results and discussion

3.1. TEM analysis

The microsurface of the catalyst samples and the size and distribution of the nanoparticles are shown in Fig. 1. As can be seen from Fig. 1(a), the surface of the pretreated MWNTs was very smooth due to the introduction of functional groups instead of defect sites on the MWNTs. In Fig. 1(b), Pd nanoparticles were dispersed onto the MWNTs, but some agglomerates could be observed, possibly attributable to the lack of surface functional

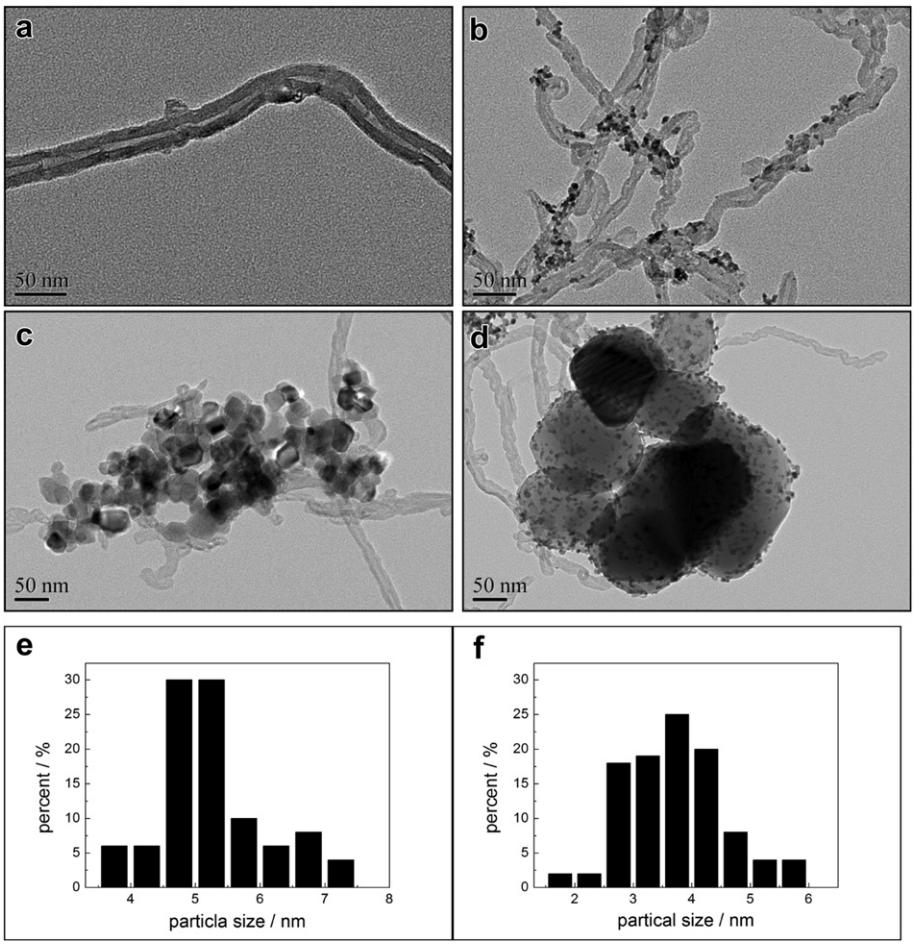

Fig. 1. TEM images of (a) MWNTs, (b) Pd/MWNTs, (c) TiO_2-MWNTs, and (d) Pd/TiO_2-MWNTs, and corresponding size distribution histograms of Pd nanoparticles in (e) Pd/MWNTs and (f) Pd/TiO_2-MWNTs.

groups on parts of the MWNTs surfaces facilitating the nucleation of Pd and subsequent particle growth [22]. From Fig. 1(c), it can be observed that the MWNTs were partially covered by TiO_2 nanoparticles with an average diameter of 20 nm. This was due to the pretreatments of MWNTs and TiO_2 nanoparticles increasing the active sites on their surfaces [23]. Interestingly, after the addition of $NaBH_4$, the TiO_2 nanoparticles aggregated and became larger and rounder in shape. In addition, the Pd nanoparticles were more homogeneously dispersed onto the TiO_2 nanoparticles and had a smaller size in the Pd/TiO_2-MWNTs than those in the Pd/MWNTs. The size distribution histograms of the Pd nanoparticles based on their TEM analysis are displayed in Fig. 1(e) and Fig. 1(f). The average sizes of the Pd nanoparticles were about 5.3 and 3.8 nm for the Pd/MWNTs and Pd/TiO_2-MWNTs, respectively. This result confirms that Pd nanoparticles become smaller after the introduction of TiO_2. Additionally, the better dispersion and small size of the Pd nanoparticles in the Pd/TiO_2-MWNTs could enable more catalytically active sites to be available for electrocatalytic reaction. In summary, these results indicated that the Pd/TiO_2-MWNTs nanocomposite was successfully synthetized and the introduction of TiO_2 promoted the dispersion of the Pd nanoparticles.

3.2. XRD analysis

The structural characteristics of the catalyst samples were observed by XRD. Fig. 2 shows the XRD patterns of Pd/TiO_2-MWNTs, Pd/MWNTs, MWNTs, TiO_2-MWNTs, and TiO_2 nanoparticles. All TiO_2 samples were anatase in phase, exhibiting major peaks at 25.3°, 37.8°, 48.0°, 53.8°, 54.9°, and 62.5° (2θ) which were assigned to the diffraction planes (101), (004), (200), (105), (211) and (204), respectively [24,25]. No diffraction peaks attributable to the rutile structure of TiO_2 were observed. Additionally,

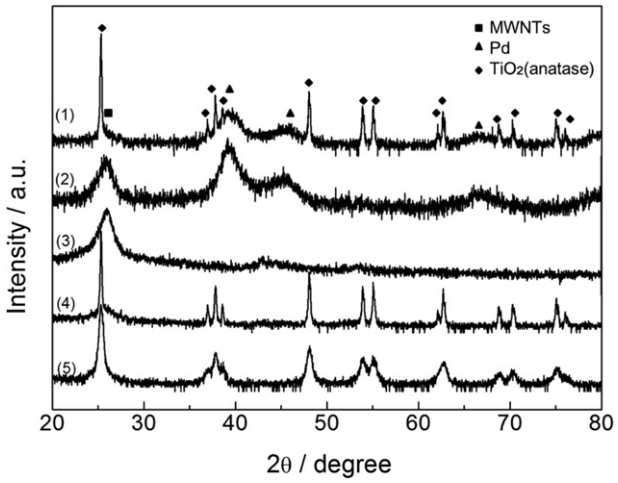

Fig. 2. XRD patterns of (1) Pd/TiO_2-MWNTs, (2) Pd/MWNTs, (3) MWNTs, (4) TiO_2-MWNTs, and (5) TiO_2 nanoparticles.

the XRD patterns of TiO_2 before and after MWNTs and Pd modifications are similar, indicating that the introduction of MWNTs and Pd made no changes to the structure of the TiO_2. In addition, the intensity of the diffraction peaks for the TiO_2 composites shows a slight increase with the addition of the MWNTs. Fig. 2(3) reveals a (002) diffraction peak at 26.4° (2θ), which is attributed to the MWNTs. This peak is overlapped by the anatase (101) diffraction of TiO_2 at 25.3° (2θ). The representative diffraction peaks for the face centered cubic crystal structure of Pd, namely (111), (200), and (220), were observed at 39.1°, 45.6°, and 66.8° (2θ) in the XRD patterns of all samples [26], demonstrating that the Pd in both Pd/MWNTs and Pd/TiO_2-MWNTs is in metallic form. Thus, the application of TiO_2 as support material played no role in influencing the cubic crystalline structure of the metallic Pd.

3.3. XPS analysis

The electronic states and surface characteristics of the catalysts were investigated by X-ray photoelectron spectroscopy (XPS). Fig. 3 shows the representative XPS spectra of TiO_2, TiO_2-MWNTs, Pd/TiO_2-MWNTs, and Pd/MWNTs. The obtained binding energies were calibrated to the C 1s (284.6 eV) peak. C 1s, O 1s, Ti 2p and Pd 3d peaks can be observed in Fig. 3(a). The concentrations of the active component Pd in the Pd/MWNTs and Pd/TiO_2-MWNTs were determined to be 15.69 and 16.20 wt%, respectively. Through the analysis of TEM images and XPS spectra of the Pd/TiO_2-MWNTs, it could be observed that the nanoparticles successfully dispersed onto the surface of TiO_2-MWNTs were Pd particles.

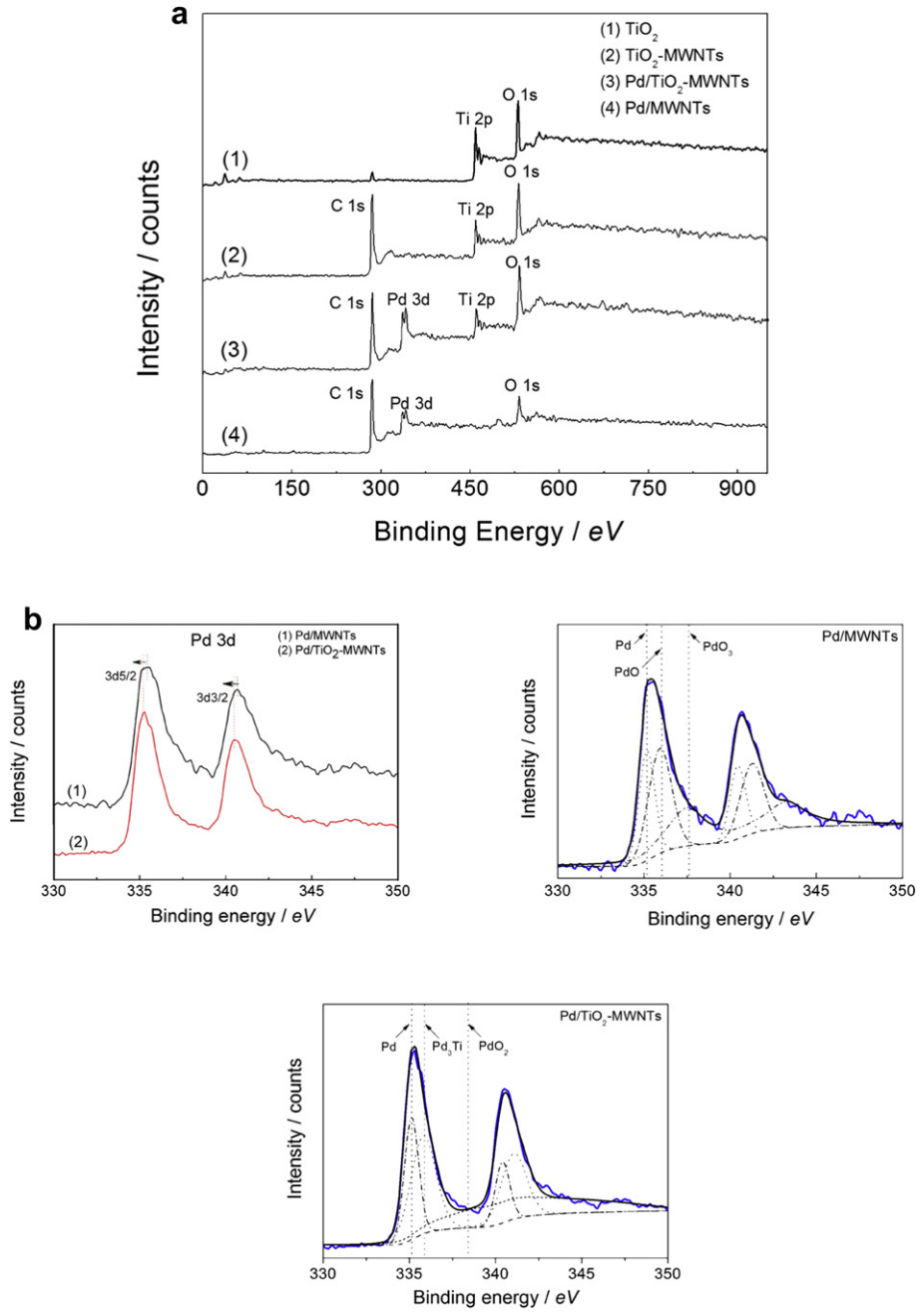

Fig. 3. (a) XPS spectra of TiO_2, TiO_2-MWNTs, Pd/TiO_2-MWNTs, and Pd/MWNTs catalysts, enlarged XPS spectra for (b) Pd 3d peak of all Pd samples and (c) Ti 2p peak of all Ti samples.

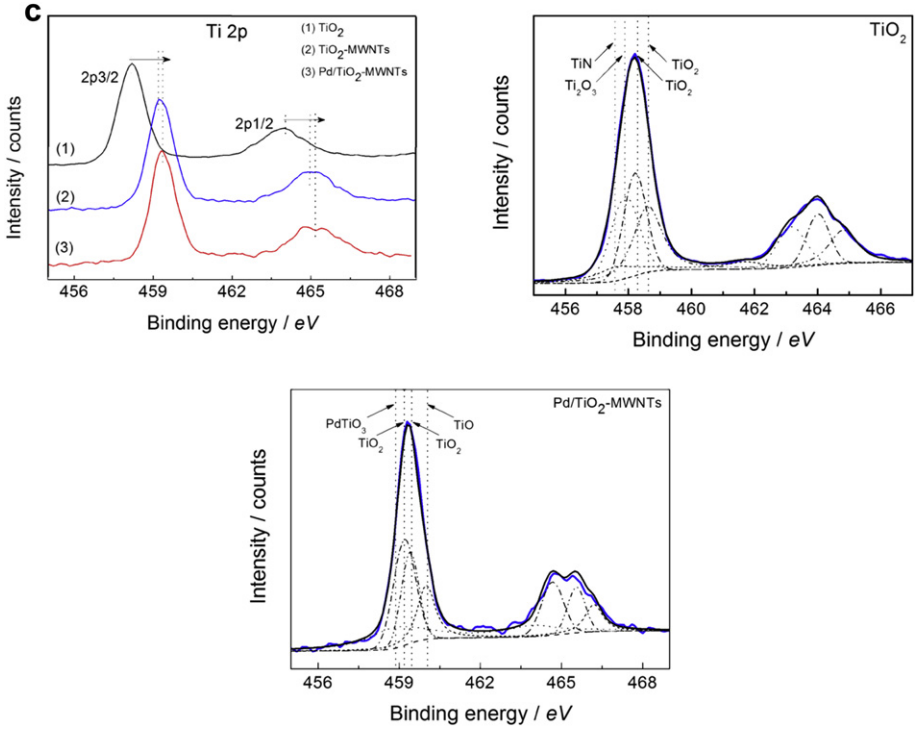

Fig. 3. (*continued*).

To understand the interactions between Pd, MWNTs, and TiO_2, the spectra of Pd 3d in Pd/MWNTs and Pd/TiO_2-MWNTs were compared. In Fig. 3(b-1), the Pd 3d spectrum of the Pd/TiO_2-MWNTs is shifted to a lower binding energy compared with the Pd/MWNTs. This implies that the Pd nanoparticles on the TiO_2-MWNTs are in a more electron rich phase than those on the MWNTs, originating from the decreasing of the band gap [27]. Deconvolutions of the Pd 3d spectra of Pd/MWNTs and Pd/TiO_2-MWNTs are shown in Fig. 3(b-2) and (b-3), respectively. In addition, the results of the deconvolution measurements are presented in Table 1, where one can clearly see the relative composition of the assigned species. The peaks at about 335.2 (Fig. 3(b-2)) and 335.1 (Fig. 3(b-3)) eV were ascribed to Pd, with corresponding relative compositions of 33.3 and 34.6%, respectively, demonstrating that most of the Pd was in the metallic state. This is in agreement with the XRD results. In addition, peaks of palladium oxide could be detected in both samples. It is also noteworthy that the peak at about 335.8 eV in the Pd/TiO_2-MWNTs spectrum was attributed to Pd_3Ti, demonstrating the occurrence of interaction between Pd and TiO_2.

Spectra of Ti 2p were constructed to investigate the TiO_2 surface characteristic in the TiO_2, TiO_2-MWNTs, and Pd/TiO_2-MWNTs samples (Fig. 3(b-1)). It was observed that the binding energy in TiO_2 is lower than that of the other two samples. This was due to the introduction of the MWNTs, which strongly interacted with the TiO_2 particles. The Ti 2p spectra of the TiO_2-MWNTs and Pd/TiO_2-MWNTs show a difference at about 465 eV, and the relative energy position of the Pd/TiO_2-MWNTs was positively shifted. This was caused by the injection of Pd nanoparticles. Deconvolutions of the Ti 2p spectra of the TiO_2-MWNTs and Pd/TiO_2-MWNTs are shown in Fig. 3(c-2) and Fig. 3(c-3). Table 2 shows the deconvolution results of the Ti 2p peaks. Most of the Ti appeared as TiO_2. The expected TiN and Ti_2O_3 peaks at about 457.6 and 457.8 eV, respectively, confirmed that the additive used (0.5 M HNO_3) had successfully modified the TiO_2 particles [28]. The peak at about 460.2 eV (Fig. 3(c-3)) belongs to TiO, demonstrating that the added $NaBH_4$ reduced part of the TiO_2. In addition, the peak at about 458.8 eV for $PdTiO_3$ demonstrates that Pd reacted with TiO_2 during the synthesis process.

3.4. Electrochemical analysis

The direct electrocatalytic behavior of Pd/MWNTs and Pd/TiO_2-MWNTs modified electrodes were investigated by cyclic voltammetry. Fig. 4(a) shows CVs of MWNTs and TiO_2-MWNTs modified electrodes in 0.5 M H_2SO_4 solution at a scan rate of 100 mV s^{-1}. Obviously, the direct dispersion of TiO_2 on the MWNTs could not improve their electrocatalytic activity (Fig. 4(a)). Fig. 4(b) shows the CVs of Pd/MWNTs and Pd/TiO_2-MWNTs in 0.5 M H_2SO_4 solution. Two pairs of peaks in the potential range −0.4–0.1 V can be distinguished in the CVs of the Pd/MWNTs and Pd/TiO_2-MWNTs, which were attributed to the absorption (oxidation peak) and desorption (reduction peak) of hydrogen. Another oxidation peak

Table 1
Distribution of Pd species and their relative composition.

Sample	Pd/MWNTs			Pd/TiO_2-MWNTs		
Assigned species	Pd	PdO	PdO_3	Pd	Pd_3Ti	PdO_2
Peak BE/eV	335.2	335.9	337.6	335.1	335.8	337.9
RC %	33.3	42.1	24.6	34.6	39.2	26.2

BE for binding energy.
RC % = relative composition %.

Table 2
Distribution of Ti species and their relative composition.

Sample	TiO_2			Pd/TiO_2-MWNTs				
Assigned species	TiN	TiO_2		Ti_2O_3	$PdTiO_3$	TiO_2		TiO
Peak BE/eV	457.6	458.3	458.6	457.8	458.8	459.0	459.2	460.2
RC %	10.5	60.4		29.1	18.2	58.5		23.3

BE for binding energy.
RC % = relative composition %.

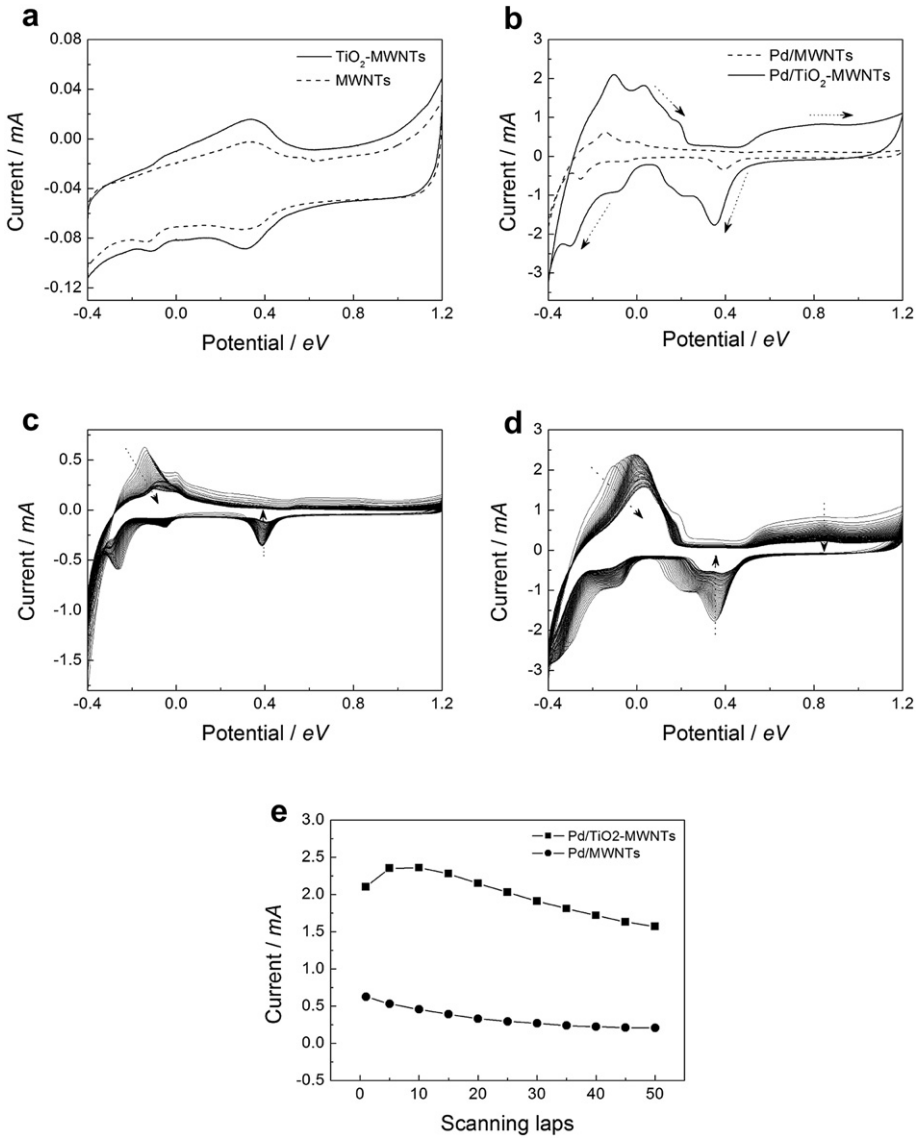

Fig. 4. Cyclic voltammograms of (a) MWNTs and TiO_2-MWNTs, and (b) Pd/MWNTs and Pd/TiO_2-MWNTs in 0.5 M H_2SO_4 at a scan rate of 100 mV s^{-1}, and cyclic voltammograms over 50 consecutive cycles of (c) Pd/MWNTs and (d) Pd/TiO_2-MWNTs in 0.5 M H_2SO_4 at a scan rate of 100 mV s^{-1} (e) the change of oxidation peak currents in the CVs of Pd/MWNTs and Pd/TiO_2-MWNTs.

and reduction peak at about 0.8 and 0.4 V, ascribed to Pd oxidation and hydrogen ion reduction, respectively, can also be observed. The electro–redox area is an important factor to measure the effectiveness of electrochemical reactions [29]. Based on the CVs in Fig. 4(b), the redox areas of both catalysts could be calculated. The electro–redox area of the Pd/TiO_2-MWNTs was found to be 5.19 times larger than that of the Pd/MWNTs, indicating that the electrocatalytic activity of the catalyst was promoted by applying TiO_2 as a support material. This result was due to the high dispersion and small size of metallic Pd nanoparticles and the function of pretreated TiO_2 which promoted the rate of the heterogeneous electro transfer. Fig. 4(c) and (d) show cyclic voltammograms over 50 consecutive scanning laps for the Pd/MWNTs and Pd/TiO_2-MWNTs electrodes, respectively. As can be seen from Fig. 4(c) and (d), the areas of the cyclic voltammograms decrease with the increasing number of cycles. This was caused by reduction of electrochemical activity sites on the surface of the modified electrode. However, after 40 cycles, the catalytic activity of the modified electrode reached a stable state. In addition, the decreasing electro–redox areas for the Pd/TiO_2-MWNTs were much smaller than those for the Pd/MWNTs, indicating that the introduction of TiO_2 nanoparticles not only promoted their electrocatalytic activity, but also enhanced their stability. Fig. 4(e) shows the oxidation peak currents of Pd/MWNTs and Pd/TiO_2-MWNTs over 50 consecutive scanning laps. It was found that the oxidation peak current of the Pd/MWNTs decreased by about 66%, while there was only about a 25% decrease for the Pd/TiO_2-MWNTs. These results confirm that the interaction between TiO_2 support and catalytic Pd nanoparticles greatly enhanced the long-term cycle durability of the catalysts. These phenomena are attributed to the unique abilities of pretreated TiO_2 nanoparticles, which provided larger superficial activity area and lowered the degradation of active surface area.

To evaluate the catalyst for application in direct formic acid fuel cells, the CVs of Pd/TiO_2-MWNTs for formic acid oxidation were measured and are shown in Fig. 5(a). For comparison, the CVs of Pd/MWNTs are also presented in Fig. 5(a). Two oxidation peaks in the forward scan and one oxidation peak in the backward scan were obtained for both Pd catalysts (Fig. 5(a)). This phenomenon is in

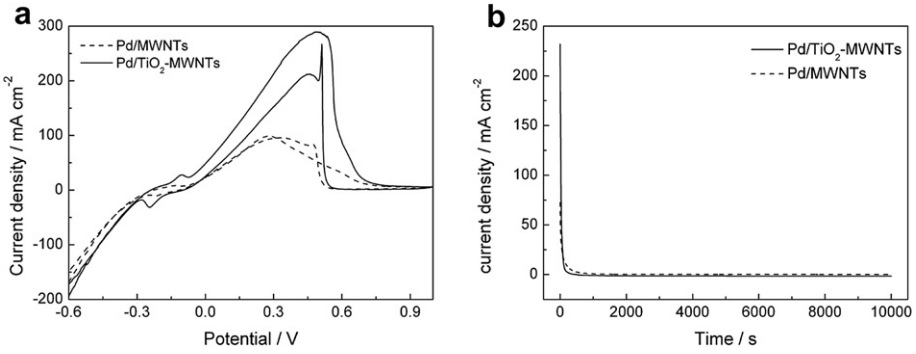

Fig. 5. (a) Cyclic voltammograms of Pd/MWNTs and Pd/TiO_2-MWNTs modified electrode in 0.5 M H_2SO_4 with 1 M HCOOH solution at a scan rate of 50 mV s^{-1}, (b) Chronoamperometric curves for Pd/MWCNT and Pd/TiO_2-MWNTs electrodes at 0.4 V for 10,000 s in the presence of 1 M HCOOH and 0.5 M H_2SO_4.

good agreement with most of the literature [21,30]. The two oxidation peaks observed during the positive scan were attributed to the following process: HCOOH → reactive intermediates → $CO_2 + 2H^+ + 2e^-$ [29,31]. The reactive intermediates play an important role in poisoning species on Pd catalysts [32]. The oxidation peak observed during the reverse scan was attributed to the reduction of surface oxides on Pd. From Fig. 5(a), it is clear that the oxidation peak current density of Pd/TiO_2-MWNTs was more than 3 times higher than that of Pd/MWNTs, indicating that the catalytic activity of Pd/TiO_2-MWNTs was better than that of Pd/MWNTs. This improved performance was due to strong integration of Pd and TiO_2 and to the pretreated TiO_2 which promoted the dispersion of Pd. In addition, the current density of the Pd/TiO_2-MWNTs catalyst was higher than those previously reported for Pd catalysts using other carbon supports as templates [33,34]. This indicated that the present Pd/TiO_2-MWNTs catalyst had great catalytic activity for formic acid oxidation.

Furthermore, the stability of the Pd/TiO_2-MWNTs catalyst was further assessed by chronoamperometry measurements (I–t curve) at 0.4 V for 10,000 s, as shown in Fig. 5(b). It was observed that the maximum current densities of Pd/MWNTs and Pd/TiO_2-MWNTs were about 72.9 and 231.4 mA cm^{-2}, respectively. Afterward, the current densities of Pd/TiO_2-MWNTs and Pd/MWNTs decreased exponentially and then remained almost constant. Evidently, the Pd/MWNTs and Pd/TiO_2-MWNTs catalysts showed good stability for formic acid oxidation. However, the high initial current densities for both Pd catalysts were not sustained over a long period. This phenomenon was caused by the absorption of reactive intermediates. The results indicated that the introduction of TiO_2 into the Pd catalyst had no effect on Pd deactivation. The Pd/TiO_2-MWNTs electrode resistance to Pd deactivation in the HCOOH acid system was inferior to results which have been reported in the literatures [35,36]. Consequently, future studies are still needed to gain a better understanding of the Pd deactivation mechanism, and subsequently improve the Pd catalysts poisoning resistance.

4. Conclusions

The intrinsic semiconductor properties of TiO_2 nanoparticles are the hurdle to their application in actual electrochemical reactions. To solve this problem, an additive (0.5 M HNO_3) was chosen to decrease the band gap and increase the electronic conductivity of the TiO_2. From analysis of TEM, XRD, and XPS results, it was found that the MWNTs were partially covered by the pretreated TiO_2, and that the Pd nanoparticles in the Pd/TiO_2-MWNTs were homogeneously dispersed on the TiO_2 nanoparticles with smaller sizes compared with those found in Pd/MWNTs. The results of electrocatalytic activity tests indicated that the application of TiO_2 nanoparticles as support material between Pd nanoparticles and MWNTs template highly improved its electrocatalytic activity and long-term cycle stability for formic acid oxidation. These results were attributed to the small size and high dispersibility of the metallic Pd crystals caused by a strong interaction between Pd and the pretreated TiO_2, and the multifunction of TiO_2 which promoted the rate of heterogeneous electron transfer. Accordingly, more studies are warranted to improve the catalytic activity of the Pd catalyst and decrease Pd deactivation.

Acknowledgments

This work was financially supported by the Natural Science Foundation of China (Grant No. 51008154), the Research Fund for the Doctoral Program of Higher Education of China (Grant No. 20090091120007), the Fundamental Research Funds for the Central Universities (Grant No. 1112021101), and the Scientific Research Foundation of Graduate School of Nanjing University (Grant No. 2012CL19).

References

[1] A. Honciuc, M. Laurin, S. Albu, M. Sobota, P. Schmuki, J. Libuda, Langmuir 26 (17) (2010) 14014–14023.
[2] T. Doi, Y. Miwa, Y. Iriyama, T. Abe, Z. Ogumi, J. Phys. Chem. C 113 (2009) 7719–7722.
[3] M.J. Lázaro, V. Celorrio, L. Calvillo, E. Pastor, R. Moliner, J. Power Sources 196 (2011) 4236–4241.
[4] W. Wei, W. Chen, J. Power Sources 204 (2012) 85–88.
[5] Y.G. Suo, L. Zhuang, J.T. Lu, Angew. Chem. Int. Ed. 46 (2007) 2862.
[6] K.J. Young, J. Youngshin, K. Seong-Keun, S. Lee, H.C. Choi, J. Mol. Catal. A-Chem. 323 (2010) 28–32.
[7] Q.Z. Jiang, X. Wu, M. Shen, Z.F. Ma, X.Y. Zhu, Catal. Lett. 124 (2008) 434–438.
[8] R.S. Hsu, D. Higgins, Z. Chen, Nanotechnology 21 (2010) 165705–165710.
[9] T. Ioroi, Z. Siroma, N. Fujiwara, S. Yamazaki, K. Yasuda, Electrochem. Commun. 7 (2005) 183.
[10] S.H. Kang, T.Y. Jeon, H.S. Kim, Y.E. Sung, W.H. Smyrl, J. Electrochem. Soc. 155 (2008) B1058.
[11] K.S. Lee, I.S. Park, Y.H. Cho, D.S. Jung, N. Jung, H.Y. Park, Y.E. Sung, J. Catal. 258 (2008) 143.
[12] L.C. Jiang, W.D. Zhang, Electroanalysis 21 (2009) 988–993.
[13] F. Peng, L.F. Cai, H. Yu, H.J. Wang, J. Yang, J. Solid State Chem. 181 (2008) 130.
[14] M. Gratzel, Nature 414 (2001) 338–344.
[15] W. Tian, H.S. Yang, X.Y. Fan, X.B. Zhang, Catal. Commun. 11 (2010) 1185–1188.
[16] L. Kavan, R. Bacsa, M. Tunckol, P. Serp, S.M. Zakeeruddin, F.L. Formal, M. Zukalova, M. Graetzel, J. Power Sources 195 (2010) 5360–5369.
[17] T.A. Saleh, V.K. Gupta, J. Colloid Interface. Sci. 371 (2012) 101–106.
[18] K. Woan, G. Pyrgiotakis, W. Sigmund, Adv. Mater. 21 (2009) 2233–2239.
[19] Y. Qin, Y. Jiang, H. Yang, X. Zhang, X. Zhou, Li Niu, W. Yuan, J. Power Sources 196 (2011) 4609–4612.
[20] V. Selvaraja, A.N. Graceb, M. Alagarc, J. Colloid Interface. Sci. 333 (2009) 254–262.
[21] G. Hu, F. Nitze, H.R. Barzegar, T. Sharifi, A. Mikołajczuk, C. Tai, A. Borodzinski, T. Wågberg, J. Power Sources 209 (2012) 236–242.
[22] D.C. Higgins, J.Y. Choi, J. Wu, J. Mater. Chem. 22 (2012) 3727.

[23] L.H. Yu, J.G. Xi, Electrochim. Acta 67 (2012) 166–171.
[24] Y. Zhao, Y. Hu, Y. Li, H. Zhang, S.W. Zhang, L.T. Qu, G.Q. Shi, L.M. Dai, Nanotechnology 21 (2010) 505702.
[25] Z. Lei, M. Zeda, O.W. Chun, Chin. J. Catal. 32 (2011) 926–932.
[26] M. Choi, C. Han, I.T. Kim, J.J. Lee, H.K. Lee, J. Shim, J. Nanosci. Nanotechnol. 11 (2011) 6420–6424.
[27] D.S. Kim, E.F.A. Zeid, Y.T. Kim, Electrochim. Acta 55 (2010) 3628–3633.
[28] X.Y. Zhang, H.P. Li, X.L. Cui, Y.H. Lin, J. Mater. Chem. 20 (2010) 2801–2806.
[29] Y.N. Jeong, M.Y. Choi, H.C. Choi, Electrochim. Acta 60 (2012) 78–84.
[30] S. Park, J. Park, Curr. Appl. Phys. 12 (2012) 1248–1251.
[31] D.M. Acosta, J.L. Garcia, L.A. Godinez, H.G. Rodríguez, L.Á. Contreras, L.G. Arriaga, J. Power Sources 195 (2010) 461–465.
[32] O. Winjobi, Z. Zhang, C. Liang, W. Li, Electrochim. Acta 55 (2010) 4217–4221.
[33] Y. Lu, W. Chen, J. Phys. Chem. C 114 (2010) 21190–21200.
[34] J. Yang, C. Tian, L. Wang, H. Fu, J. Mater. Chem. 21 (2011) 3384–3390.
[35] H. Zhao, J. Yang, L. Wang, C. Tian, B. Jiang, H. Fu, Chem. Commun. 47 (2011) 2014–2016.
[36] T.T. Cheng, E.L. Gyenge, J. Appl. Electrochem. 39 (2009) 1925–1938.